nature
structural &
molecular biology

The refined structure of nascent HDL reveals a key functional domain for particle maturation and dysfunction

Zhiping Wu[1,2], Matthew A Wagner[3], Lemin Zheng[1,6], John S Parks[4], Jacinto M Shy III[3], Jonathan D Smith[1,5], Valentin Gogonea[2,3] & Stanley L Hazen[1,2,5]

The cardioprotective function of high-density lipoprotein (HDL) is largely attributed to its ability to facilitate transport of cholesterol from peripheral tissues to the liver. However, HDL may become dysfunctional through oxidative modification, impairing cellular cholesterol efflux. Here we report a refined molecular model of nascent discoidal HDL, determined using hydrogen-deuterium exchange mass spectrometry. The model reveals two apolipoprotein A1 (apoA1) molecules arranged in an antiparallel double-belt structure, with residues 159–180 of each apoA1 forming a protruding solvent-exposed loop. We further show that this loop, including Tyr166, a preferred target for site-specific oxidative modification within atheroma, directly interacts with and activates lecithin cholesterol acyl transferase. These studies identify previously uncharacterized structural features of apoA1 in discoidal HDL that are crucial for particle maturation, and elucidate a structural and molecular mechanism for generating a dysfunctional form of HDL in atherosclerosis.

Plasma HDL cholesterol and apoA1 levels are inversely correlated with the risk for coronary artery disease[1–3]. The effects of both genetic and direct infusion–induced changes in apoA1 levels in humans and animal models confirm a potent antiatherosclerotic activity of apoA1 (refs. 1–6). A major presumed mechanism for apoA1's anti-atherogenic properties is its role in removal of cholesterol from peripheral tissues to the liver, a process termed reverse cholesterol transport (RCT). RCT is complex and involves numerous steps, including the efflux of cholesterol from peripheral cells to nascent discoidal HDL and the maturation of discoidal HDL into a cholesterol ester–laden spherical particle. ApoA1, the major protein component of HDL, is crucial both in allowing the transfer of cholesterol and phospholipids from peripheral tissues to nascent discoidal HDL and in activation of lecithin-cholesteryl acyl transferase (LCAT), an enzyme essential for cholesterol esterification and maturation of HDL[1–3].

In addition to plasma levels of HDL, the functional properties of the particle also seem to be crucial in determining its overall cardioprotective effects. For example, HDL isolated from subjects with either cardiovascular disease or systemic inflammatory disorders seems to have been rendered dysfunctional, so that it has proinflammatory and proatherosclerotic biological activities[7–9]. Moreover, results from recent clinical studies of HDL-elevating therapies underscore that not just quantity but also function of the lipoprotein is important[10–12]. These studies also highlight the need to better define, at the molecular and structural levels, the features of HDL that facilitate efflux and maturation activities during RCT, as well as the potential mechanisms for generating dysfunctional forms of HDL.

ApoA1 oxidation has recently been identified as one mechanism for generating dysfunctional HDL. For example, analyses of HDL recovered from either atherosclerotic plaque or plasma from subjects with cardiovascular disease have revealed that apoA1 is a preferred target for oxidative modification, resulting in loss of its capacity to promote cholesterol efflux[13–17]. Furthermore, mass spectrometric analyses of the recovered apoA1 have revealed post-translational modifications consistent with increased exposure to nitrating and chlorinating oxidants, presumably produced by leukocyte-derived myeloperoxidase (MPO), an enzyme implicated in the pathogenesis of cardiovascular disease[13,15,16]. Thus, impairment in the cholesterol-efflux functions of apoA1 in atherosclerotic plaque after oxidation represents one mechanism underlying the generation of dysfunctional HDL. Whether HDL can be rendered dysfunctional by interference with other steps in the RCT pathway, such as particle maturation, remains unknown. Moreover, the structural features of apoA1 necessary to support alternative steps of the RCT pathway, such as LCAT activation and discoidal HDL maturation, are unclear.

[1]Department of Cell Biology, Cleveland Clinic, 9500 Euclid Avenue, NE-10, Cleveland, Ohio 44195, USA. [2]Center for Cardiovascular Diagnostics and Prevention, Cleveland Clinic, 9500 Euclid Avenue, NE-10, Cleveland, Ohio 44195, USA. [3]Chemistry Department, Cleveland State University, Cleveland, Ohio 44115, USA. [4]Department of Pathology/Section on Lipid Sciences, Wake Forest University, School of Medicine, Winston-Salem, North Carolina 27157, USA. [5]Department of Cardiovascular Medicine, Cleveland Clinic, 9500 Euclid Avenue, NE-10, Cleveland, Ohio 44195, USA. [6]Present address: PrognostiX, Inc.,10265 Carnegie Avenue, Cleveland, Ohio 44106, USA. Correspondence should be addressed to S.L.H. (hazens@ccf.org).

Received 30 March; accepted 2 July; published online 5 August 2007; doi:10.1038/nsmb1284

The X-ray crystal structure of full-length 'lipid-free' apoA1 has recently been reported[18]. Although a wealth of biophysical approaches have provided insights into structural features of apoA1 within discoidal HDL[19–24], high-resolution structures of apoA1 within either nascent discoidal HDL or spheroidal HDL forms are not yet available. Here we have developed a refined structural model of human discoidal HDL to further elucidate the structural features of HDL that facilitate RCT and to provide a framework for better understanding of potential molecular mechanisms for generating dysfunctional forms of HDL.

RESULTS

Refined molecular model of nascent discoidal HDL

Upon lipidation, apoA1 undergoes structural changes to form nascent discoidal HDL. To investigate these structural changes, we generated recombinant discoidal HDL for comparison with lipid-free full-length human apoA1. Physical, biochemical and cross-linking analyses of the nascent discoidal HDL preparation confirmed the presence of a functional (with respect to cholesterol efflux and LCAT activities) particle of approximately 96 Å diameter, with two apoA1 molecules per particle and overall apoA1/phospholipid/cholesterol stoichiometry of 1:109:8.6 (mol/mol/mol, **Supplementary Fig. 1** online). To quantitatively examine the conformational changes of apoA1 upon lipid binding, we used a nonperturbing biophysical method, hydrogen-deuterium exchange tandem mass spectrometry. With this method, the degree of deuterium incorporation can be sensitively and specifically measured at amide protons in overlapping peptides and their collision-induced fragments at nearly residue-level resolution; thus, each amino acid residue throughout the primary protein sequence can theoretically serve as an intrinsic quantifiable probe of protein solvent accessibility and conformation.

Hydrogen-deuterium exchange analyses of solvent accessibility within 48 pairs of peptic peptides across the entire sequence of apoA1, corresponding to ~95% coverage for both the lipid-free and discoidal HDL forms, revealed several features of both forms (**Fig. 1**). First, lipid-free apoA1, except for residues 14–18, 90–111 and 148–180, is highly solvent exposed, as demonstrated by a high degree of deuterium incorporation. In comparison, apoA1 within discoidal HDL had numerous regions with markedly lower deuterium incorporation, consistent with residues in these regions being buried within or abutting lipid and/or protein. The spectral region illustrated in **Figure 1a** represents the isotopic cluster of a peptide that shows the typical behavior seen in comparisions of peptides from lipid-free apoA1 with those from nascent HDL, before and after incubation with >99% deuterated phosphate buffer. Within nascent HDL, Arg213–Leu219 peptide experiences 40% less deuterium incorporation compared with the same peptide in the lipid-free apoA1 (**Fig. 1b,c**), consistent with diminished solvent accessibility. In contrast, residues 159–180 of apoA1 within discoidal HDL show large increases in hydrogen-deuterium exchange upon lipid binding, to nearly 100% solvent accessibility (**Fig. 1a**, right, and **Fig. 1c**).

A refined molecular model of discoidal HDL in solution was generated using the previously reported double-belt model (also called the belt model)[20] as an initial template. Computational modeling involved 2,830 steps of energy minimization. The calculation of deuterium exchange probabilities was performed while satisfying the multiple new constraints imposed by the measured deuterium incorporation data, in combination with the reported cross-linking constraints (**Supplementary Table 1** online and ref. 22), the overall particle dimensions derived from light-scattering studies and the expected particle composition (**Supplementary Fig. 1**). This process resulted in a stable refined solvated model, named the 'solar-flares' model (**Fig. 2**). Similar to the belt model[20], in the solar-flares model two chains of apoA1 are stacked antiparallel, with helix 5 of each

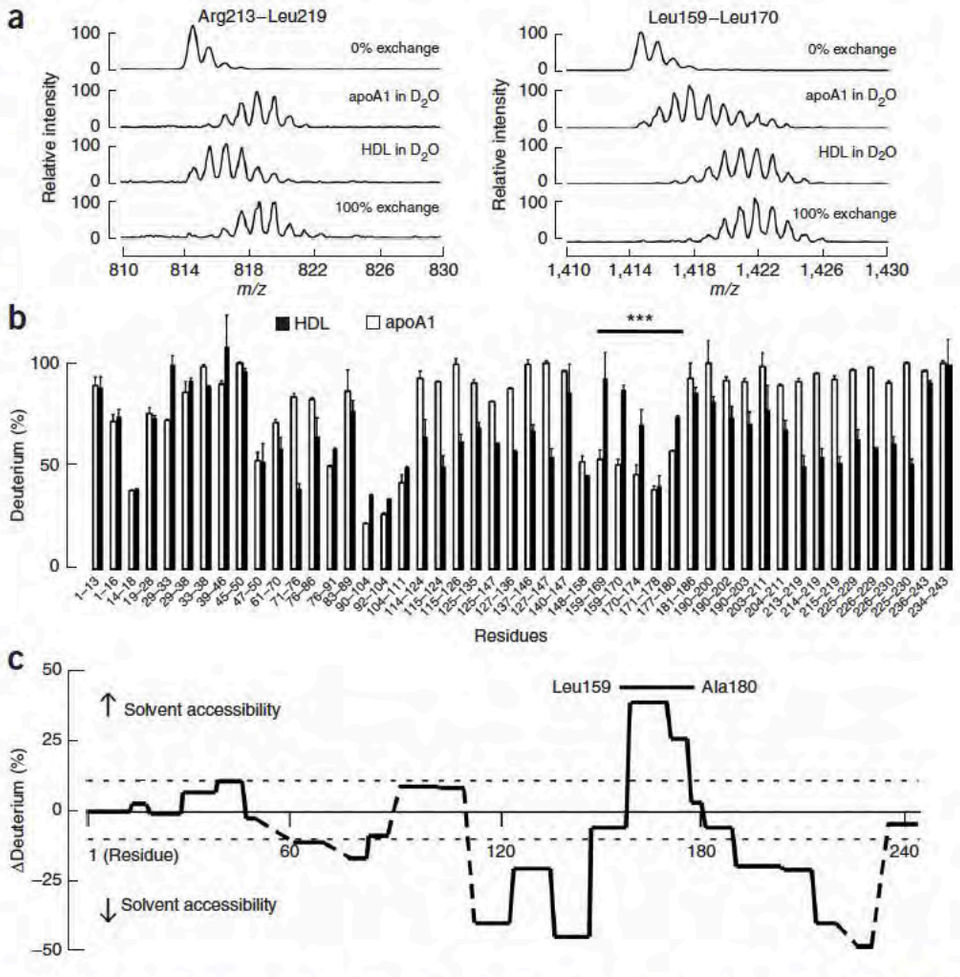

Figure 1 Solvent accessibility of lipid-free apoA1 and apoA1 within recombinant human discoidal HDL, revealed by hydrogen-deuterium exchange mass spectrometry. (**a**) Left, isotopic clusters of a typical peptic peptide (Arg213–Leu219) of apoA1, whose solvent accessibility upon lipid association in recombinant human discoidal HDL was lower than in lipid-free apoA1. Right, isotopic clusters of a peptic peptide (Leu159–Leu170) that uniquely showed increased deuterium incorporation (solvent accessibility) upon lipid association in discoidal HDL. Each panel contains four spectra of apoA1: no deuterium labeling (0% exchange), lipid-free apoA1 in D_2O, nascent HDL in D_2O, and 100% deuterium exchange. (**b**) Deuterium incorporation percentage for individual peptic peptides of apoA1 in its lipid-free (open bar) and discoidal HDL (filled bar) forms. (**c**) Percent differences between lipid-free apoA1 and apoA1 in nascent HDL, with regard to deuterium incorporation into peptic peptides. Dotted lines mark 10% differences. All results are expressed as means from three independent experiments; error bars show s.d.

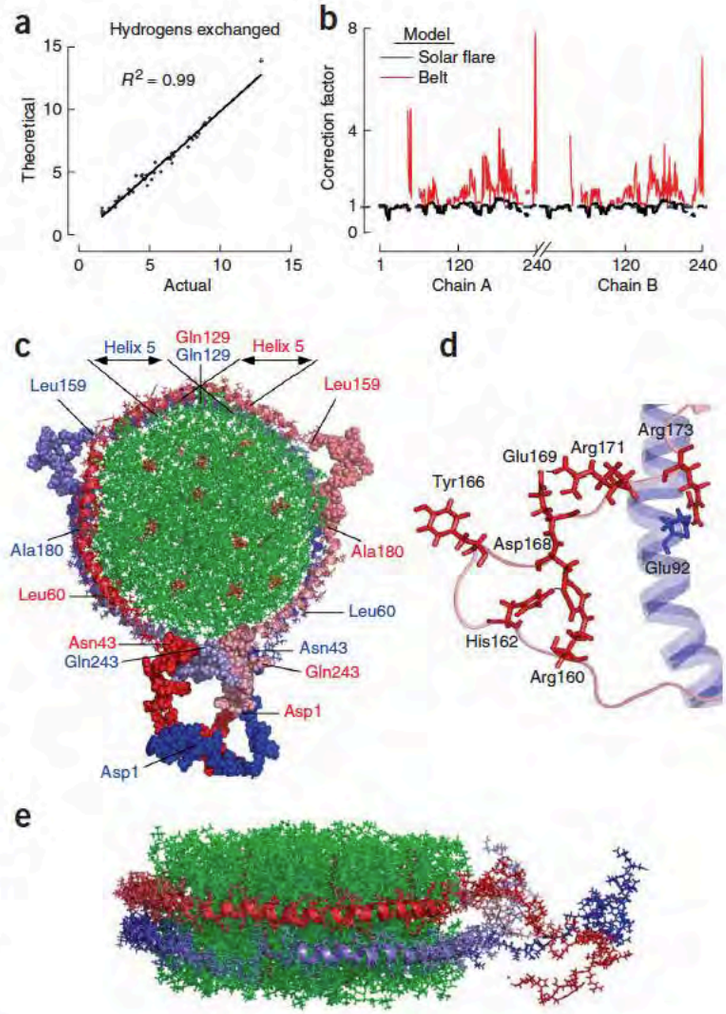

Figure 2 The solar-flares model of discoidal HDL. (**a**) The experimentally measured (actual) number of deuterium atoms incorporated into individual peptic peptides of apoA1 in discoidal HDL is correlated with the amount of deuterium predicted to be accessible for hydrogen-deuterium exchange by the solar-flares model (theoretical). (**b**) The goodness of fit of the solar-flares model and the belt model[20] at the residue level. Incorporation of deuterium into individual residues (at positions plotted on *x*-axis) was measured in peptic peptides of apoA1 in discoidal HDL where possible. The correction factor on the *y*-axis represents the multiplier needed to adjust the theoretical deuterium incorporation to match the value experimentally determined by hydrogen-deuterium exchange mass spectrometry. Dotted blue line represents a correction factor of 1 (no difference between theoretical and actual values). (**c**) Top view of the solar-flares model of discoidal HDL, shown with antiparallel stacked double-belt apoA1 architecture. One apoA1 chain (red, N terminus; pink, C terminus) encircles the discoidal HDL particle clockwise, while a second apoA1 chain (dark blue, N terminus; light blue, C terminus) encircles it counterclockwise. Green, phospholipids; orange, cholesterol molecules. (**d**) Close-up view of the highly solvent-exposed loop segment corresponding to apoA1 residues 159–180, in discoidal HDL. Residues involved in salt bridges and Tyr166 are indicated. (**e**) Side view of the solar-flares model of discoidal HDL, showing predicted α-helical secondary structures.

apoA1 overlapping. The N termini of apoA1 are absent in the belt model, as it is based on the crystal structure of an N-terminally truncated apoA1 mutant[20]. In contrast, the N termini of apoA1 form a globular domain in the solar-flares model, with residues 14–18 of one apoA1 molecule interacting with residues 14–18 of the other apoA1 molecule. The C termini of both apoA1 molecules also interact with each other, and the most distal C-terminal residues of each, 236–243, are relatively exposed to the solvent. The solar-flares model derives its name from the protruding loops corresponding to apoA1 residues 159–180 in both the α and β chains (**Fig. 2c,d**). The loop conformation appears to be stabilized by several salt bridges (**Fig. 2d**). Tyr166, a preferred site of apoA1 oxidative modification in human atherosclerotic plaque[15], protrudes from the distal end of the loop (**Fig. 2d**).

Figure 2a shows the goodness of fit ($R^2 = 0.99$) of the solar-flares model to the experimental data. **Figure 2b** illustrates the quality of the model at the amino acid–residue level, where the probability correction factor (plotted on the *y*-axis) represents the multiplier needed to adjust the theoretical deuterium incorporation of individual residues based on the solar-flares model so that it matches what was actually experimentally determined. This shows that the conformation predicted from the solar-flares model is a substantial improvement on that of the belt model. Recently, two alternative belt models have been proposed on the basis of cross-linking studies: one with a head-to-head hairpin loop structure (the hairpin model)[22] and another where the N terminus of apoA1 loops back to enable cross-linking observed between Lys12 and Lys182 (the N-terminal hairpin model)[23]. We attempted further refinements to the solar-flares model by imposing secondary structural features from either the hairpin model or the N-terminal hairpin model on the solar-flares model. This, however, resulted in inferior models (**Supplementary Tables 1** and **2** online). Notably, even in these alternative models, inclusion of the deuterium-incorporation data as a constraint universally led to HDL models in which residues 159–180 of each apoA1 chain form protruding solvent-exposed loops.

apoA1 residues Leu159–Leu170 and Tyr166 activate LCAT

One obvious question surrounding apoA1's unusual solvent-exposed loop (residues 159–180) is what function, if any, this structure supports. We noted that among 46 reported missense mutations of human apoA1, 17 reduce its capacity to activate LCAT, and many of these mutations are clustered around the loop in question (**Fig. 3a**)[25]. Moreover, it has previously been suggested that residues carrying negative charge in this region of apoA1 may be involved in LCAT interaction and activation[26]. To test whether the highly solvent-exposed loop region of nascent HDL directly interacts with LCAT for its activation, we compared deuterium incorporation throughout apoA1 within discoidal HDL in the presence and absence of human LCAT. Notably, incubation of LCAT with discoidal HDL resulted in substantial protection of deuterium incorporation in only one small contiguous region of apoA1, particularly within the peptide Leu159–Leu170 (**Fig. 3b–d**). Similar results were observed when discoidal HDL and LCAT individually were first incubated in D_2O, then combined and diluted 25-fold in an H_2O buffer (the deuterium-hydrogen 'off exchange' experiment; data not shown).

Figure 3b represents the isotopic envelope of peptide Leu159–Leu170 and a representative alternative peptide before and after incubation of LCAT with nascent HDL in D_2O. Most of the peptic peptides of apoA1 in nascent HDL had similar solvent accessibility with or without LCAT binding (**Fig. 3c**). Only two regions changed conformation considerably (>10% change in deuterium exchange): the putative apoA1-LCAT interaction site (Leu159–Leu170) and C-terminal residues 213–230, which showed slightly increased solvent accessibility with unknown biological significance. These results suggest a physical interaction between LCAT and the solvent-exposed loop comprised by Leu159–Leu170 of apoA1 in the lipoprotein.

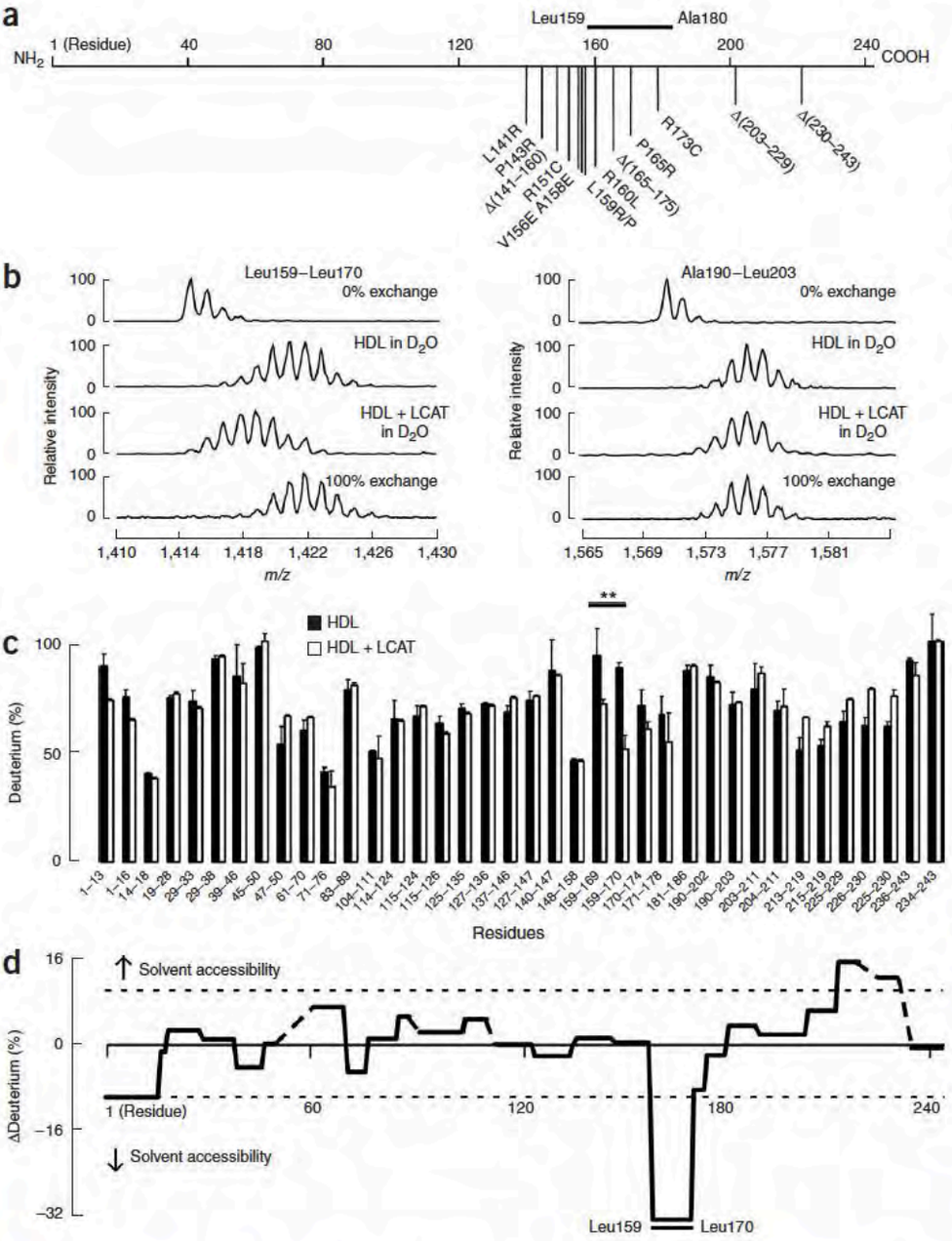

Figure 3 Residues Leu159–Leu170 of apoA1 in discoidal HDL directly interact with LCAT. (**a**) Positions of mutations in apoA1 known to affect LCAT activation, showing their proximity to the apoA1 loop that is highly solvent-exposed in discoidal HDL. (**b**) Left, mass spectra (as in **Fig. 1a**) of Leu159–Leu170, the only peptic peptide of apoA1 in discoidal HDL that shows a substantial change in deuterium incorporation in the presence of LCAT. Right, mass spectra of a characteristic control peptide of apoA1 (Ala190–Leu203) in discoidal HDL that shows no effect of LCAT on deuterium incorporation. (**c**) Percent deuterium incorporation of exchangeable protons within individual peptic peptides of apoA1 in discoidal HDL, in the absence (filled bar) or presence (open bar) of LCAT. (**d**) Percent differences in deuterium incorporation of individual peptic peptides of apoA1 in discoidal HDL, in the absence or presence of LCAT. Dotted lines mark 10% differences. All results are expressed as means from three independent experiments; error bars show s.d.

To independently confirm a direct interaction between the apoA1 Leu159–Leu170 loop in nascent HDL and LCAT, we performed peptide competition assays. Incubation of LCAT–discoidal HDL mixtures with a molar excess of a synthetic peptide corresponding to the putative apoA1 LCAT-binding loop (Leu159–Leu170) substantially inhibited LCAT activity (58% inhibition; $P < 0.001$), as measured by cholesterol ester formation (**Fig. 4a**), and to a lesser extent LCAT binding to nascent HDL (20% inhibition; $P < 0.03$, not shown). The effect on LCAT activation is specific to this peptide, as demonstrated by the lack of inhibition after co-incubation of excess control peptide (Ala190–Leu203), corresponding to an adjacent region in apoA1 involved in MPO interaction within HDL[13].

Maturation of discoidal HDL requires apoA1 Tyr166

Recently, apoA1 has been identified as a selective target for MPO-catalyzed oxidation in human atherosclerotic plaque and plasma, which impairs HDL-mediated cholesterol efflux activity of the lipoprotein particle and is associated with increased risk of cardiovascular disease[13]. Proteomic studies have revealed that chlorination and nitration of Tyr166 of apoA1 recovered from human atherosclerotic lesions is the most abundant site-specific modification detected in the lipoprotein[15], but its functional consequences remain unknown. Indeed, in subsequent studies in which all seven apoA1 tyrosines were mutated to phenylalanines, the mutated apoA1 had full cholesterol efflux activity yet remained sensitive to MPO-catalyzed oxidative inactivation, suggesting that tyrosine modification is not responsible for loss of cholesterol efflux activity in the oxidized apoA1[14]. Upon inspection of the solar-flares model, we were struck by the observation that apoA1 Tyr166 in discoidal HDL is located within the LCAT interaction loop (Leu159–Leu170) and thus might be involved in LCAT activation and particle maturation. Moreover, the model predicts the presence of several salt bridges within the loop and adjacent apoA1 belt residues, which would generate a stable secondary structure in which Tyr166 remains fully solvent exposed at the proximal tip of the loop (**Fig. 2d**), potentially positioning this aromatic residue for interaction with LCAT. To test this hypothesis, we used recombinant mutant (Y166F)apoA1 to generate discoidal HDL and examined LCAT activity. Over 70% reduction in LCAT activity ($P < 0.001$) was reproducibly observed in discoidal HDL preparations with the (Y166F)apoA1 mutant, compared with recombinant wild-type human apoA1 (**Fig. 4b**). In contrast, the (Y166F)apoA1 mutant retained full ABCA1-dependent cholesterol efflux activity (**Fig. 4c**). Thus, the phenoxyl group of apoA1 Tyr166 within discoidal HDL facilitates LCAT activation and particle maturation, a pivotal step in RCT.

HDL maturation is impaired by MPO-catalyzed oxidation

Up to 50% of HDL particles recovered from human atherosclerotic aorta in some subjects contain oxidative modification of an apoA1 tyrosine residue[13], and Tyr166 is the most prevalent site of modification found in proteomics studies of apoA1 recovered from human atherosclerotic lesions[15]. Therefore, we tested the hypothesis that

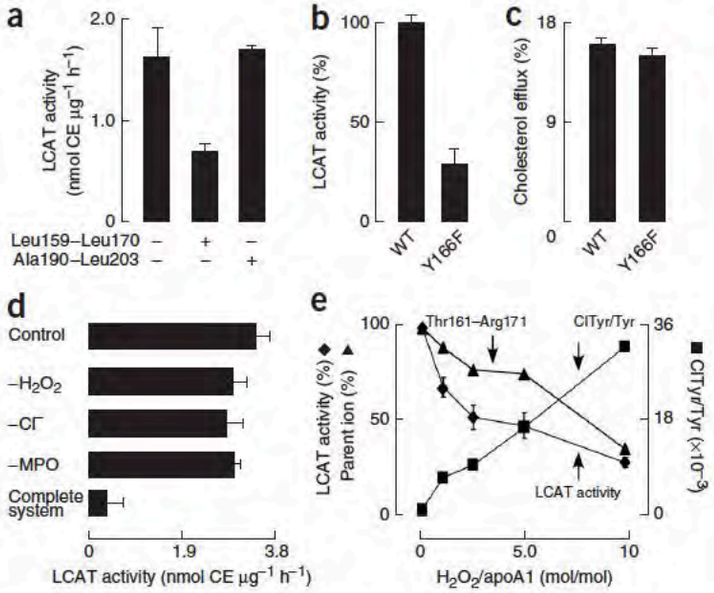

Figure 4 Peptide Leu159–Leu170 and Tyr166 of apoA1 are important for the activation of LCAT and are selectively targeted for MPO-catalyzed oxidative inactivation under physiological conditions. (**a**) Preincubation of LCAT with a molar excess of the synthetic peptide corresponding to apoA1 residues Leu159–Leu170, but not alternative control peptides (data for Ala190–Leu203 is shown), inhibits LCAT activity in the presence of discoidal HDL. CE, cholesterol ester. (**b**) LCAT activity upon incubation with comparable amounts of discoidal HDL containing either full-length recombinant human apoA1 or the (Tyr166Phe)apoA1 mutant. (**c**) Total cholesterol efflux activity of human recombinant apoA1 or (Tyr166Phe)apoA1 mutant, when added to cholesterol-loaded and 8-Br-cAMP–treated RAW264.7 cells. (**d**) Exposure of discoidal HDL to increasing amounts of oxidants generated by MPO in the MPO-H_2O_2-Cl^- system results in parallel losses of LCAT activity and of the tryptic peptide (Thr161–Arg171) corresponding to the solvent-exposed loop, and a corresponding increase in apoA1 chlorotyrosine (ClTyr/Tyr) content. All results are expressed as means ± s.d. from at least three independent experiments.

oxidative modification of apoA1 impairs HDL particle maturation by inhibiting apoA1-dependent LCAT activation. Exposure of nascent HDL to physiological concentrations of a complete MPO-H_2O_2-Cl^- system (67 nM MPO, 100 μM H_2O_2 and 100 mM NaCl) almost completely eliminated the ability of the lipoprotein particle to activate LCAT (**Fig. 4d**). Inhibition required each component of the MPO-H_2O_2-Cl^- system, consistent with a requirement that apoA1 be exposed to the MPO-generated oxidant HOCl to render HDL dysfunctional for promotion of LCAT activity. The dose-response curve for oxidative inhibition of HDL-dependent LCAT activation (**Fig. 4e**) shows nearly parallel loss of LCAT activity and disappearance of the original tryptic peptide (Thr161–Arg171) overlapping the apoA1-LCAT interaction loop (Leu159–Leu170), with a corresponding increase in apoA1 chlorotyrosine content (**Fig. 4e**). Together, these results indicate that oxidation of apoA1 within the apoA1-LCAT interaction loop (Leu159–Leu170), particularly at residue Tyr166, results in selective inhibition of LCAT-catalyzed cholesterol esterification, a crucial mediator of HDL particle maturation.

DISCUSSION

Despite the well-established link between HDL cholesterol level and atherosclerosis risk, the inability to directly visualize high-resolution structures of HDL through crystallography has hampered a detailed understanding of the particle's structure. Similarly, the precise structural and molecular underpinnings of the interactions between apoA1 in HDL and other participants in RCT remain unknown. Several models of nascent HDL have been proposed, with the majority of the evidence supporting a double-belt model for the overall architecture of apoA1 (refs. 19–23). NMR spectroscopy analyses of a discoidal HDL preparation suggest an overall helical secondary structure of lipidated apoA1 and a backbone proline conformation consistent with a belt model[19,27]. The present studies substantially clarify the structure of discoidal HDL. They also provide insights as to how the structure of apoA1 within HDL begets its function in a crucial step of the RCT pathway, LCAT activation and particle maturation. Incorporation of quantitative solvent-accessibility data for apoA1 at nearly residue-level resolution from hydrogen-deuterium exchange tandem mass spectrometry has permitted substantial refinement of the computational model, as well as enabling us to quantitatively evaluate the fit between the model and experimental data at both the peptide level and the residue level of resolution.

Figure 5 illustrates the solar-flares model overall, highlighting the apoA1-LCAT interaction site, a feature crucial for particle maturation as well as for generating a dysfunctional form of HDL in human atherosclerotic plaque. Also shown are the recently identified MPO interaction site on apoA1 (Ala190–Leu203)[13] and the sites of the two most abundant post-translational modifications observed in apoA1 recovered from human atherosclerotic plaque, Tyr166 and Tyr192 (ref. 15).

The present studies suggest the following model. Freshly synthesized lipid-poor apoA1 is highly dynamic and solvent exposed. Upon lipidation, apoA1 generates a discoidal HDL particle composed of two apoA1 molecules arranged in an antiparallel double-belt structure, similar in global architecture to that previously proposed[20]. The greater resolution of the solar-flares model reveals that residues 159–180 of each apoA1 chain protrude from the body of the particle as solvent-exposed loops. Each of these loops, including Tyr166, functions as an LCAT interaction site and is crucial for LCAT activation. Finally, HDL that diffuses into the artery wall, particularly at a site of atherosclerotic plaque, seems to encounter a hostile environment where MPO-generated chlorinating oxidants and nitric oxide–derived oxidants promote site-specific oxidation of apoA1 at Tyr166 (ref. 15). The resultant dysfunctional HDL particle is much less capable of activating LCAT. Such a particle, if modified in the form of nascent or discoidal HDL, would function like a maturation-arrested HDL particle.

ApoA1 is recognized as the major activator of LCAT in nascent discoidal HDL during RCT. However, the mechanism by which apoA1 facilitates cholesterol esterification and particle maturation is not completely understood. Deletion of residues Met148–Gly186 of apoA1 forms a mutant apoA1 with markedly reduced capacity to activate LCAT[28,29]. Moreover, mutation of several charged residues in the region historically referred to as helix 6 (Pro143–Ala164) results in marked reductions in LCAT activity, which have been interpreted to imply a role for these residues in ionic interactions between apoA1 and LCAT[26,29]. However, the solar-flares model predicts several potential intraloop salt-bridges, involving Arg160, His162, Asp168, Glu169 and Arg171, among others. Thus, rather than ionic interactions with LCAT, many of these residues may form essential intramolecular salt bridges within the apoA1-LCAT interaction loop, necessary for stabilizing a secondary structural conformation required for LCAT activation. It is also possible that the conformation of the apoA1 loop (residues 159–180) formed in nascent HDL not only facilitates direct interactions between apoA1 and LCAT but also helps

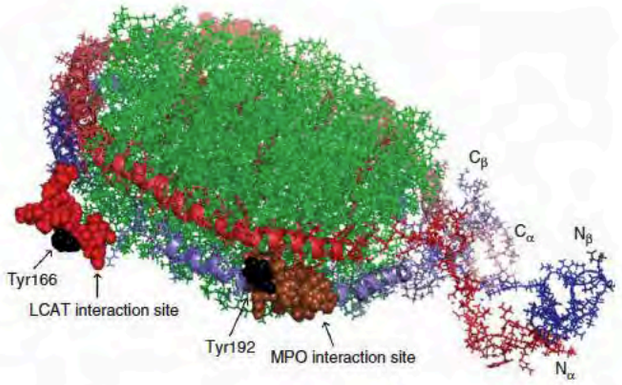

Figure 5 Refined solar-flares model of discoidal HDL, illustrating sites of known protein-protein interactions and site-specific oxidative modifications reported within human atherosclerotic plaque. The LCAT interaction site (residues 159–170, filled red) and MPO-binding site (residues 190–203, filled brown) are shown. The sites of the two most abundant site-specific oxidative modifications found in apoA1 recovered from human atherosclerotic lesions (Tyr166 and Tyr192)[15] are in black. The remaining color scheme is as in **Figure 2c**. The N and C termini of the apoA1 α and β chains in HDL are also shown.

present the exposed phospholipid and free cholesterol to LCAT as substrate. Indeed, a second region (residues 90–114) of apoA1 in nascent HDL showed modest enhancement in solvent exposure upon lipid binding (**Fig. 1b,c**). In the solar-flares model, residues 90–114 of one apoA1 chain are paired with the apoA1-LCAT interaction loop of the other apoA1 chain. Thus, formation of the loop on one apoA1 chain may weaken the interhelical interaction between the apoA1 chains, allowing the segment in the second apoA1 more solvent exposure. One consequence of this may be analogous to starting the unzipping of a zipper, as it would potentially allow cholesterol ester to be inserted between the phospholipid leaflets into a growing particle core. Indeed, monoclonal antibodies that specifically bind apoA1 residues 95–121 in discoidal HDL inhibit LCAT activation[30]. The present results provide a structural rationale for these observations: steric interference in productive LCAT interaction at residues 159–170 of the alternative apoA1 chain.

Historically, lipid-bound apoA1 has been thought to be made up of α-helical segments of 22 or 11 residues, interspersed between α-helix–breaking prolines[31]. Whereas the belt model basically follows this prescription, the solar-flares model is less circular, mainly owing to the constraints imposed on the shape so that it is consistent with cross-links reported in subsequent studies[22]. In terms of intermolecular salt bridges, the belt and solar-flares models are hardly distinguishable: the loss of one intermolecular salt bridge (Lys96-Glu169) present only in the belt model is compensated by the presence of two additional intramolecular salt bridges (Arg160-Asp168 and His162-Asp168) in the LCAT-binding loop, or flare, of the solar-flares model. A further intermolecular salt bridge in the solar-flares model, Asp20-Arg10, may facilitate association of residues 14–18 of the two chains. Both the original belt model[20] and the solar-flares model have a pitch of 1 1/3 residues per turn. The α-helical content of lipid-bound truncated apoA1, calculated from circular dichroism data, is 78% ± 1% for apoA1 Δ(1–43)[32]. When the N termini (assumed to be unfolded on the basis of marked hydrogen-deuterium exchange) are included, the estimated α-helical content decreases to 64%, in agreement with the estimated content for the solar-flares model (59%).

The concept of an intramolecular hairpin within apoA1 of discoidal HDL is not unprecedented. A movable 'hinge' domain has been proposed to exist within the region historically called helices 5, 6 and 7, and this domain may form an intramolecular hairpin, potentially expanding to help apoA1 accommodate changing particle size with varied lipid content[21]. Resonance energy transfer studies using engineered apoA1 variants have similarly suggested the presence of an extended loop structure in the vicinity of residues 134–145 (ref. 33). By using each amide proton throughout the polypeptide chain as an intrinsic quantitative nonperturbing probe of apoA1 conformation, we have confirmed the concept of an intramolecular loop but refined its predicted location to a different region.

Of note, our results indicate the functional consequence of MPO-catalyzed oxidation of apoA1 Tyr166, a post-translational modification that is abundant on apoA1 in human atherosclerotic aorta but whose functional significance was previously unknown[15]. Functional analysis of the (Y166F)apoA1 mutant confirmed that the *para*-hydroxyphenyl moiety of Tyr166 is required for LCAT activation by apoA1 within discoidal HDL. We have previously reported high levels of chlorinated Tyr166 in apoA1 recovered from human coronary artery lesions[15], consistent with a catalytic role for MPO in oxidative inactivation of HDL within human lesions. Even when exposure to MPO-generated oxidants was low, we found that Tyr166 is selectively targeted for oxidation, with corresponding loss in LCAT activity (**Fig. 4e**). Assuming that chlorination of only one Tyr166 per HDL particle is needed to inhibit activation of LCAT, our data suggest that chlorination of apoA1 Tyr166 accounts for a maximum of 70% of the observed inhibition in LCAT activity after exposure of HDL to the MPO-H_2O_2-Cl^- system. Thus, other residues besides Tyr166 in the apoA1-LCAT interaction loop may also serve as targets for oxidation by the MPO-H_2O_2-Cl^- system and contribute to the inactivation of the HDL particle.

On the basis of the data reported here, it is tempting to speculate that therapeutic strategies designed to interrupt MPO-apoA1 interactions, MPO activity and generation of nitric oxide–derived oxidants may be of benefit. However, the net impact of LCAT inactivation in the atherosclerotic plaque remains unclear, as data from animal models are conflicting[34–36]. In clinical studies, subjects heterozygous for *LCAT* gene mutations associated with diminished activity showed increased carotid intima thickness compared with family controls, suggesting that a reduction in LCAT activity may indeed be proatherogenic in humans[37,38].

Recent interest has focused on therapeutic strategies aimed at raising HDL levels for potential atheroprotective benefit[2,6,10–12]. However, a growing body of evidence supports the notion that not only the quantity but also the functional properties of the HDL particle are important for its overall impact on cardiovascular disease[1,8–12]. The present studies provide insights into discoidal HDL structure and function. They also delineate a molecular mechanism for generating a maturation-arrested dysfunctional form of HDL within human atheroma. These studies thus provide further support for mechanistic links between specific oxidative pathways, inflammation and atherosclerosis.

METHODS

Recombinant human apoA1 and apoA1 mutants, and reconstituted nascent HDL. Human apoA1 was purchased from Biodesign. Recombinant full-length human apoA1 was expressed in *Escherichia coli* and isolated as described[14]. The Y166F point mutation was made using the QuikChange mutagenesis kit (Stratagene) and confirmed by DNA sequencing. Reconstituted nascent HDL was prepared using sodium cholate dialysis[39] at an initial molar ratio of 100:10:1 1-palmitoyl-2-oleoyl-*sn*-glycero-3-phosphocholine (POPC)/cholesterol/isolated apoA1. HDL particles were characterized using cholesterol efflux assays

with cholesterol-laden RAW264.7 cells in the presence or absence of 8-Br-cAMP, light scattering, nondenaturing PAGE and SDS-PAGE after cross-linking[22,23].

Hydrogen-deuterium exchange and mass spectrometric analyses. Hydrogen-deuterium exchange tandem mass spectrometry studies were done essentially as described[13] (see **Supplementary Methods** online). Before data collection, conditions were optimized to minimize back exchange, so that the maximal deuterium incorporated in the fully exchanged peptides compared well with the theoretical maximum of a fully exposed peptide (all peptides shown differ from the theoretical peptide by $<25\%$, with an average difference of $<10\%$–15%).

Molecular modeling of discoidal HDL. The initial solar-flares model of discoidal HDL was built with Modeller[40] using the published double-belt model of discoidal HDL as the template[20] with the addition of the N-terminal residues 1–43 of apoA1. DeepView in Swiss-PDBViewer[41] was used for refinement of the solar-flares model to accommodate chemical cross-link constraints and the insertion of additional POPC molecules and cholesterol into the model (to match the molar ratio of 100:10:1 for POPC/cholesterol/apoA1). Then we used our own analysis program, DEXANAL (data not shown), to calculate per-residue deuterium exchange probabilities. These probabilities were summed to obtain the theoretically determined deuterium exchange values, which were then compared with the experimental deuterium exchange incorporation data (see **Supplementary Methods** for more detailed information). Structure coordinates are available from the Protein Model DataBase (see below) and from S.L.H. upon request.

Myeloperoxidase modifications and assessment of LCAT activity. MPO-mediated modification reactions were carried out by exposing either isolated apoA1 or discoidal HDL preparations to an MPO-H_2O_2-Cl^- system, as described[13]. Human recombinant LCAT was expressed in and purified from CHO cells as reported[42]. LCAT activity was assayed after incubation with reconstituted discoidal ^{3}H-cholesterol–labeled HDL, and ^{3}H-cholesteryl ester formation was quantified as described[43]. In peptide competition studies, synthetic peptides Leu159–Leu170 and Ala190–Leu203 of apoA1 (20:1 peptide/apoA1, mol/mol) were individually mixed with LCAT before incubation with HDL.

Statistic analysis. Statistical significance of differences was determined by Student's *t*-test. *P*-values for statistical differences are reported when $P < 0.05$. All experimental results are expressed as means ± s.d. from at least three independent replicate experiments.

Accession codes. Protein Model DataBase (http://mi.caspur.it/PMDB/main.php): Coordinates have been deposited with accession code PM0074956.

Note: Supplementary information is available on the Nature Structural & Molecular Biology website.

ACKNOWLEDGMENTS

This work was supported by US National Institutes of Health grants P01 HL076491, P50 HL77107, HL70621, HL066082, 1R15 GM070469-01, P01 HL049373 and HL 054176, and the Cleveland Clinic Foundation General Clinical Research Center (M01 RR018390). Z.W. was partially supported by an American Heart Association Fellowship Award.

AUTHOR CONTRIBUTIONS

Z.W. and S.L.H. designed all studies and prepared the manuscript. Z.W. carried out all biochemical studies. V.G., M.A.W. and J.M.S. performed computational modeling. J.D.S. and J.S.P. assisted in generation of recombinant proteins. L.Z. and Z.W. performed all proteomic studies.

COMPETING INTERESTS STATEMENT

The authors declare no competing financial interests.

Published online at http://www.nature.com/nsmb/

Reprints and permissions information is available online at http://npg.nature.com/reprintsandpermissions

1. Barter, P.J. & Rye, K.A. Relationship between the concentration and antiatherogenic activity of high-density lipoproteins. *Curr. Opin. Lipidol.* **17**, 399–403 (2006).
2. Rader, D.J. Mechanisms of disease: HDL metabolism as a target for novel therapies. *Nat. Clin. Pract. Cardiovasc. Med.* **4**, 102–109 (2007).
3. Assmann, G. & Gotto, A.M., Jr. HDL cholesterol and protective factors in atherosclerosis. *Circulation* **109**, III8–III14 (2004).
4. Plump, A.S., Scott, C.J. & Breslow, J.L. Human apolipoprotein A-I gene expression increases high density lipoprotein and suppresses atherosclerosis in the apolipoprotein E-deficient mouse. *Proc. Natl. Acad. Sci. USA* **91**, 9607–9611 (1994).
5. Nissen, S.E. *et al.* Effect of recombinant ApoA-I Milano on coronary atherosclerosis in patients with acute coronary syndromes: a randomized controlled trial. *J. Am. Med. Assoc.* **290**, 2292–2300 (2003).
6. Linsel-Nitschke, P. & Tall, A.R. HDL as a target in the treatment of atherosclerotic cardiovascular disease. *Nat. Rev. Drug Discov.* **4**, 193–205 (2005).
7. Ansell, B.J. *et al.* Inflammatory/antiinflammatory properties of high-density lipoprotein distinguish patients from control subjects better than high-density lipoprotein cholesterol levels and are favorably affected by simvastatin treatment. *Circulation* **108**, 2751–2756 (2003).
8. Nicholls, S.J., Zheng, L. & Hazen, S.L. Formation of dysfunctional high-density lipoprotein by myeloperoxidase. *Trends Cardiovasc. Med.* **15**, 212–219 (2005).
9. Kontush, A. & Chapman, M.J. Functionally defective high-density lipoprotein: a new therapeutic target at the crossroads of dyslipidemia, inflammation, and atherosclerosis. *Pharmacol. Rev.* **58**, 342–374 (2006).
10. Tall, A.R. CETP inhibitors to increase HDL cholesterol levels. *N. Engl. J. Med.* **356**, 1364–1366 (2007).
11. Nissen, S.E. *et al.* Effect of torcetrapib on the progression of coronary atherosclerosis. *N. Engl. J. Med.* **356**, 1304–1316 (2007).
12. Kastelein, J.J. *et al.* Effect of torcetrapib on carotid atherosclerosis in familial hypercholesterolemia. *N. Engl. J. Med.* **356**, 1620–1630 (2007).
13. Zheng, L. *et al.* Apolipoprotein A-I is a selective target for myeloperoxidase-catalyzed oxidation and functional impairment in subjects with cardiovascular disease. *J. Clin. Invest.* **114**, 529–541 (2004).
14. Peng, D.Q. *et al.* Tyrosine modification is not required for myeloperoxidase-induced loss of apolipoprotein A-I functional activities. *J. Biol. Chem.* **280**, 33775–33784 (2005).
15. Zheng, L. *et al.* Localization of nitration and chlorination sites on apolipoprotein A-I catalyzed by myeloperoxidase in human atheroma and associated oxidative impairment in ABCA1-dependent cholesterol efflux from macrophages. *J. Biol. Chem.* **280**, 38–47 (2005).
16. Bergt, C. *et al.* The myeloperoxidase product hypochlorous acid oxidizes HDL in the human artery wall and impairs ABCA1-dependent cholesterol transport. *Proc. Natl. Acad. Sci. USA* **101**, 13032–13037 (2004).
17. Shao, B. *et al.* Tyrosine 192 in apolipoprotein A-I is the major site of nitration and chlorination by myeloperoxidase, but only chlorination markedly impairs ABCA1-dependent cholesterol transport. *J. Biol. Chem.* **280**, 5983–5993 (2005).
18. Ajees, A.A., Anantharamaiah, G.M., Mishra, V.K., Hussain, M.M. & Murthy, H.M. Crystal structure of human apolipoprotein A-I: insights into its protective effect against cardiovascular diseases. *Proc. Natl. Acad. Sci. USA* **103**, 2126–2131 (2006).
19. Li, Y., Kijac, A.Z., Sligar, S.G. & Rienstra, C.M. Structural analysis of nanoscale self-assembled discoidal lipid bilayers by solid-state NMR spectroscopy. *Biophys. J.* **91**, 3819–3828 (2006).
20. Segrest, J.P. *et al.* A detailed molecular belt model for apolipoprotein A-I in discoidal high density lipoprotein. *J. Biol. Chem.* **274**, 31755–31758 (1999).
21. Maiorano, J.N., Jandacek, R.J., Horace, E.M. & Davidson, W.S. Identification and structural ramifications of a hinge domain in apolipoprotein A-I discoidal high-density lipoproteins of different size. *Biochemistry* **43**, 11717–11726 (2004).
22. Silva, R.A., Hilliard, G.M., Li, L., Segrest, J.P. & Davidson, W.S. A mass spectrometric determination of the conformation of dimeric apolipoprotein A-I in discoidal high density lipoproteins. *Biochemistry* **44**, 8600–8607 (2005).
23. Bhat, S., Sorci-Thomas, M.G., Alexander, E.T., Samuel, M.P. & Thomas, M.J. Intermolecular contact between globular N-terminal fold and C-terminal domain of ApoA-I stabilizes its lipid-bound conformation: studies employing chemical cross-linking and mass spectrometry. *J. Biol. Chem.* **280**, 33015–33025 (2005).
24. Thomas, M.J., Bhat, S. & Sorci-Thomas, M.G. The use of chemical cross-linking and mass spectrometry to elucidate the tertiary conformation of lipid-bound apolipoprotein A-I. *Curr. Opin. Lipidol.* **17**, 214–220 (2006).
25. Zannis, V.I., Chroni, A. & Krieger, M. Role of apoA-I, ABCA1, LCAT, and SR-BI in the biogenesis of HDL. *J. Mol. Med.* **84**, 276–294 (2006).
26. Alexander, E.T. *et al.* Apolipoprotein A-I helix 6 negatively charged residues attenuate lecithin-cholesterol acyltransferase (LCAT) reactivity. *Biochemistry* **44**, 5409–5419 (2005).
27. Mishra, V.K. *et al.* Association of a model class A (apolipoprotein) amphipathic alpha helical peptide with lipid: high resolution NMR studies of peptide.lipid discoidal complexes. *J. Biol. Chem.* **281**, 6511–6519 (2006).
28. Minnich, A. *et al.* Site-directed mutagenesis and structure-function analysis of the human apolipoprotein A-I. Relation between lecithin-cholesterol acyltransferase activation and lipid binding. *J. Biol. Chem.* **267**, 16553–16560 (1992).
29. Sorci-Thomas, M.G., Curtiss, L., Parks, J.S., Thomas, M.J. & Kearns, M.W. Alteration in apolipoprotein A-I 22-mer repeat order results in a decrease in lecithin:cholesterol acyltransferase reactivity. *J. Biol. Chem.* **272**, 7278–7284 (1997).
30. Banka, C.L., Bonnet, D.J., Black, A.S., Smith, R.S. & Curtiss, L.K. Localization of an apolipoprotein A-I epitope critical for activation of lecithin-cholesterol acyltransferase. *J. Biol. Chem.* **266**, 23886–23892 (1991).
31. Borhani, D.W., Rogers, D.P., Engler, J.A. & Brouillette, C.G. Crystal structure of truncated human apolipoprotein A-I suggests a lipid-bound conformation. *Proc. Natl. Acad. Sci. USA* **94**, 12291–12296 (1997).

32. Rogers, D.P. *et al.* Truncation of the amino terminus of human apolipoprotein A-I substantially alters only the lipid-free conformation. *Biochemistry* **36**, 288–300 (1997).
33. Martin, D.D., Budamagunta, M.S., Ryan, R.O., Voss, J.C. & Oda, M.N. Apolipoprotein A-I assumes a "looped belt" conformation on reconstituted high density lipoprotein. *J. Biol. Chem.* **281**, 20418–20426 (2006).
34. Furbee, J.W., Jr., Sawyer, J.K. & Parks, J.S. Lecithin:cholesterol acyltransferase deficiency increases atherosclerosis in the low density lipoprotein receptor and apolipoprotein E knockout mice. *J. Biol. Chem.* **277**, 3511–3519 (2002).
35. Lambert, G. *et al.* Analysis of glomerulosclerosis and atherosclerosis in lecithin cholesterol acyltransferase-deficient mice. *J. Biol. Chem.* **276**, 15090–15098 (2001).
36. Lee, R.G. *et al.* Plasma cholesteryl esters provided by lecithin:cholesterol acyltransferase and acyl-coenzyme a:cholesterol acyltransferase 2 have opposite atherosclerotic potential. *Circ. Res.* **95**, 998–1004 (2004).
37. Hovingh, G.K. *et al.* Compromised LCAT function is associated with increased atherosclerosis. *Circulation* **112**, 879–884 (2005).
38. Hovingh, G.K. *et al.* Inherited disorders of HDL metabolism and atherosclerosis. *Curr. Opin. Lipidol.* **16**, 139–145 (2005).
39. Matz, C.E. & Jonas, A. Micellar complexes of human apolipoprotein A-I with phosphatidylcholines and cholesterol prepared from cholate-lipid dispersions. *J. Biol. Chem.* **257**, 4535–4540 (1982).
40. Sali, A. & Blundell, T.L. Comparative protein modelling by satisfaction of spatial restraints. *J. Mol. Biol.* **234**, 779–815 (1993).
41. Guex, N. & Peitsch, M.C. SWISS-MODEL and the Swiss-PdbViewer: an environment for comparative protein modeling. *Electrophoresis* **18**, 2714–2723 (1997).
42. Chisholm, J.W., Gebre, A.K. & Parks, J.S. Characterization of C-terminal histidine-tagged human recombinant lecithin:cholesterol acyltransferase. *J. Lipid Res.* **40**, 1512–1519 (1999).
43. Parks, J.S., Gebre, A.K. & Furbee, J.W. Lecithin-cholesterol acyltransferase. Assay of cholesterol esterification and phospholipase A2 activities. *Methods Mol. Biol.* **109**, 123–131 (1999).